*Article*

# Boosting Magnetoelectric Effect in Polymer-Based Nanocomposites

**Alexander Omelyanchik [1,2], Valentina Antipova [1], Christina Gritsenko [1], Valeria Kolesnikova [1], Dmitry Murzin [1], Yilin Han [3], Andrei V. Turutin [4,5], Ilya V. Kubasov [4], Alexander M. Kislyuk [4], Tatiana S. Ilina [4], Dmitry A. Kiselev [4], Marina I. Voronova [4], Mikhail D. Malinkovich [4], Yuriy N. Parkhomenko [4], Maxim Silibin [6,7,8], Elena N. Kozlova [3], Davide Peddis [2,9], Kateryna Levada [1], Liudmila Makarova [1,10], Abdulkarim Amirov [1,11,*] and Valeria Rodionova [1,*]**

1 REC Smart Materials and Biomedical Applications, Immanuel Kant Baltic Federal University, 236041 Kaliningrad, Russia; asomelyanchik@kantiana.ru (A.O.); vantipova1@kantiana.ru (V.A.); christina.byrka@gmail.com (C.G.); vgkolesnikova1@kantiana.ru (V.K.); dvmurzin@yandex.ru (D.M.); elevada@kantiana.ru (K.L.); la.loginova@physics.msu.ru (L.M.)
2 Department of Chemistry and Industrial Chemistry (DCIC), University of Genova, 16146 Genova, Italy; davide.peddis@unige.it
3 Biomedical Centre, Department of Neuroscience, Uppsala University, 751 24 Uppsala, Sweden; yilin.han@neuro.uu.se (Y.H.); elena.kozlova@neuro.uu.se (E.N.K.)
4 Laboratory of Physics of Oxide Ferroelectrics and Department of Materials Science of Semiconductors and Dielectrics, National University of Science and Technology MISiS, 119049 Moscow, Russia; aturutin92@gmail.com (A.V.T.); kubasov.ilya@gmail.com (I.V.K.); akislyuk94@gmail.com (A.M.K.); ilina.tatina@gmail.com (T.S.I.); dm.kiselev@gmail.com (D.A.K.); mvoron@bk.ru (M.I.V.); malinkovich@yandex.ru (M.D.M.); parkh@rambler.ru (Y.N.P.)
5 Department of Physics and I3N, University of Aveiro, 3810-193 Aveiro, Portugal
6 Institute of Advanced Materials and Technologies, National Research University of Electronic Technology "MIET", 124498 Moscow, Russia; sil_m@mail.ru
7 Institute for Bionic Technologies and Engineering, I.M. Sechenov First Moscow State Medical University, 119991 Moscow, Russia
8 Scientific-Manufacturing Complex "Technological Centre" Shokin Square, House 1, Bld. 7, Zelenograd, 124498 Moscow, Russia
9 Institute of Structure of Matter–CNR, Monterotondo Stazione, 00016 Rome, Italy
10 Faculty of Physics, Lomonosov Moscow State University, 1-2 Leninskie Gory, 119234 Moscow, Russia
11 Amirkhanov Institute of Physics of Dagestan Federal Research Center, Russian Academy of Sciences, Makhachkala 367003, Russia
* Correspondence: amiroff_a@mail.ru (A.A.); vvrodionova@kantiana.ru (V.R.)

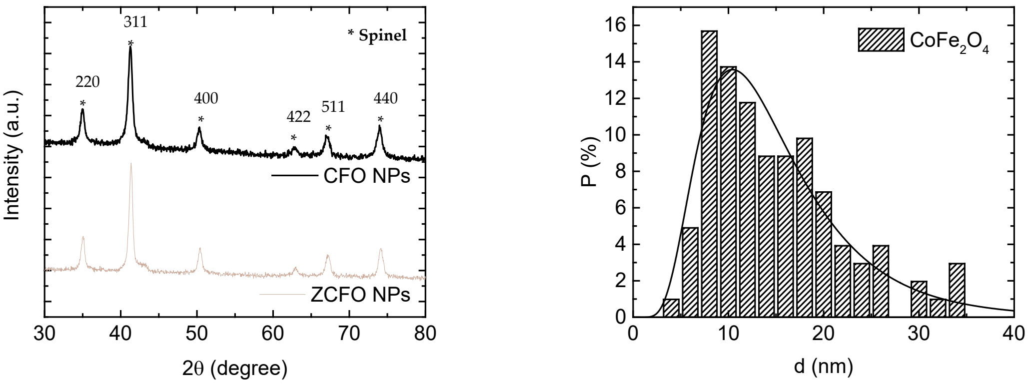


(**a**) (**b**)

**Figure S1.** (**a**) XRD pattern of $CoFe_2O_4$ and $Zn_{0.25}Co_{0.75}Fe_2O_4$ NPs; (**b**) TEM micrograph and size distribution of $CoFe_2O_4$ NPs.

Magnetic interparticle interactions were investigated by measuring the isothermal remanent magnetization (IRM) and the direct current demagnetization (DCD) [1,2].

$M_{IRM}$(H) was measured on the demagnetized sample applying a set of increasing fields (up to 10 kOe), removing them and recording the remanent magnetization after each iteration. $M_{DCD}$(H) was measured saturating first the sample, applying a set of increasing reverse fields and recording the remanent magnetization after each iteration. According to the Stoner–Wohlfarth model for an assembly of non-interacting randomly oriented MNPs with uniaxial anisotropy the two remanent magnetization curves are correlated by the following equation: $M_{DCD}(H) = 1 - 2 \cdot M_{IRM}(H)$. The effect of interparticle interactions can be evaluated by the Kelly equation [3]:

$$\Delta M(\mathrm{H}) = M_{\mathrm{DCD}}(\mathrm{H}) - 1 + 2 \cdot M_{\mathrm{IRM}}(H) \quad (1)$$

where ΔM allows one to estimate the level of interactions. ΔM = 0 for an ideal situation with the absence of interactions. A negative value indicates the predominance of dipolar interactions, whereas a positive value indicates the predominance of exchange interactions. CFO powder sample shows a negative deviation with the intensity of about ~0.1 that suggests that in powder sample the interparticle dipolar interactions are dominant.

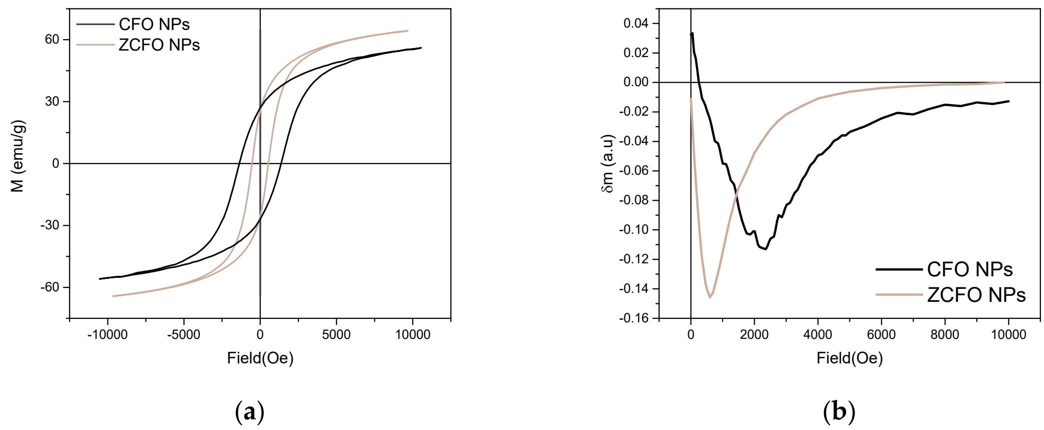


**Figure S2.** (**a**) Room temperature (~300 K) M-H loop (**b**) ΔM-plot of $CoFe_2O_4$ and $Zn_{0.25}Co_{0.75}Fe_2O_4$ NPs in form of powder.

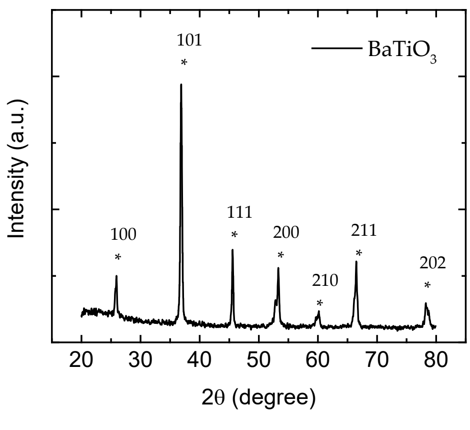


**Figure S3.** XRD pattern of $BaTiO_3$ particles.

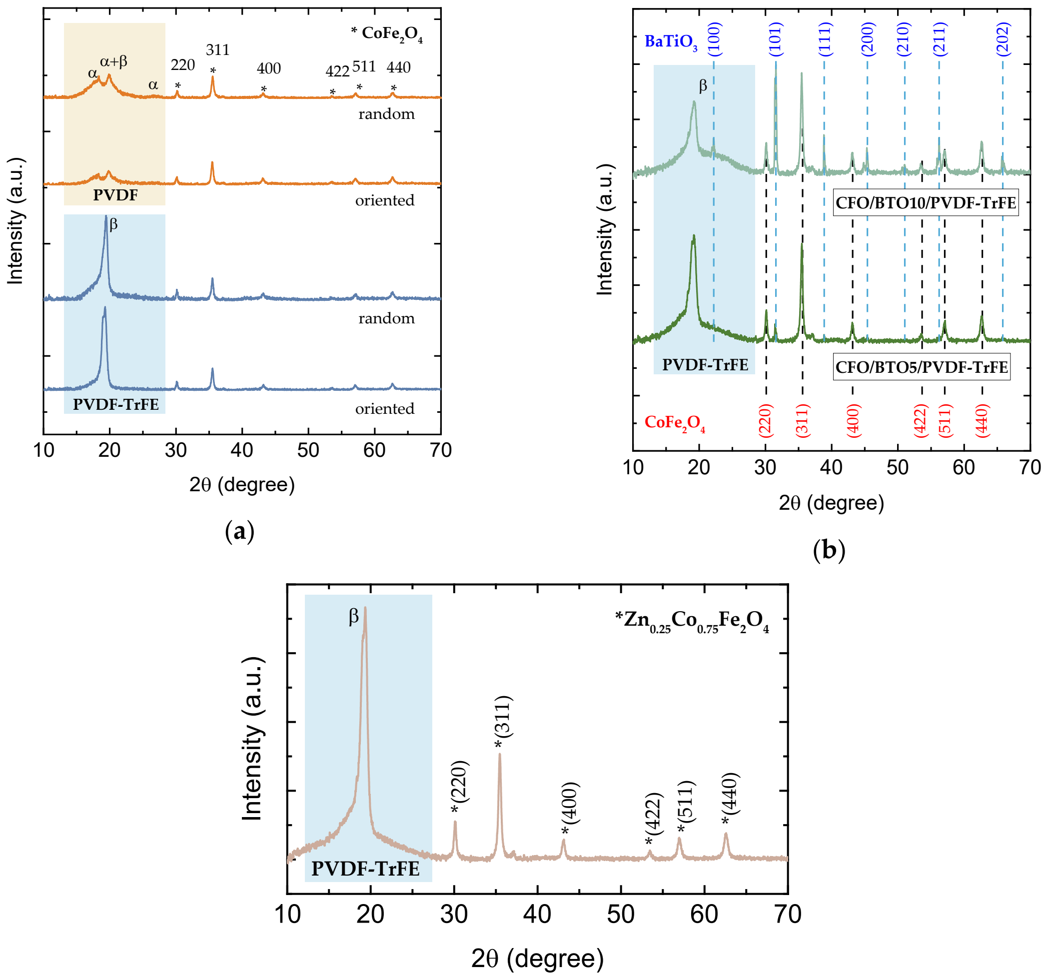


(c)

**Figure S4.** Comparison of XRD patterns for (**a**) random and oriented CFO/PVDF and CFO/PVDF-TrFE nanocomposites; (**b**) nanocomposites with 5 and 10% of $BaTiO_3$ particles; **(c)** ZCFO/PVDF-TrFE nanocomposite.

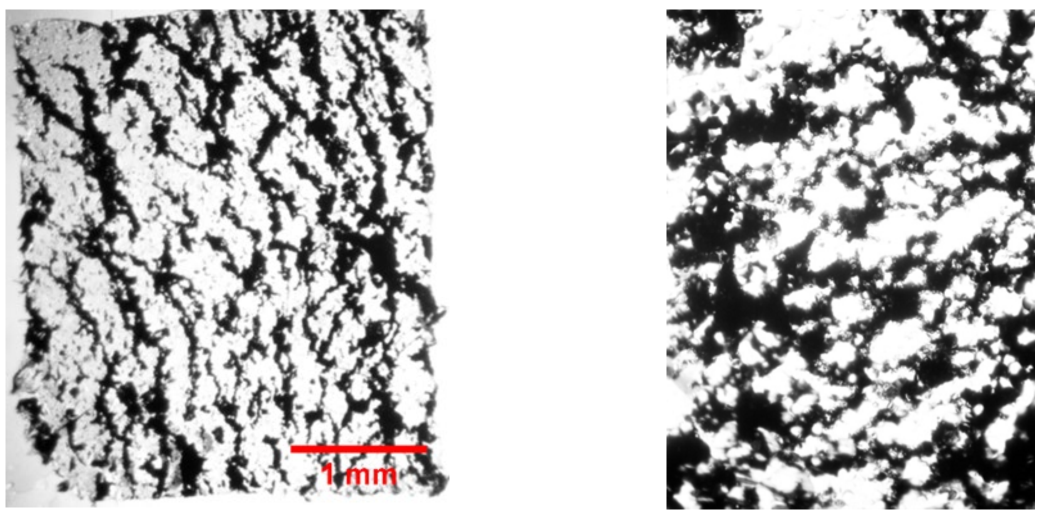


**(a)** **(b)**

**Figure S5.** Optical images of aligned clusters of CFO NPs in **(a)** PVDF-TrFE and **(b)** PVDF polymers.

The pore depth was estimated using the WSxM software [4]. Pore depth histograms were plotted using flood functions. By choosing the function "Find holes", it is possible to display all points below a certain height. By default WSxM sets flooding images by using the topography image and showing holes in different colours and holes with a height larger than the one selected here will neither be displayed nor considered during calculus. Next, a function was used to create a histogram of height. The maximum height histogram shows a histogram of the maximum value of the difference between the cutoff height and the point's height.

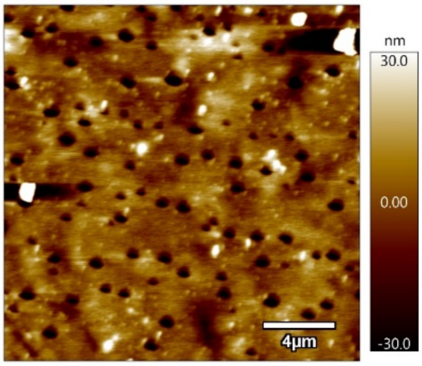


**(a)** Rms = 21 nm

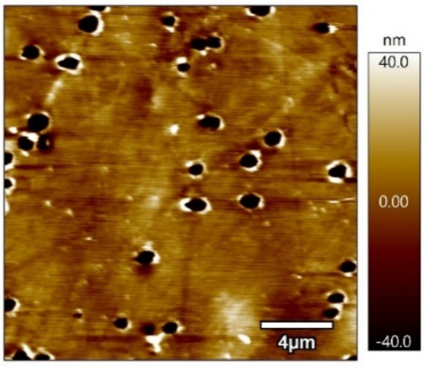


**(b)** Rms = 33 nm

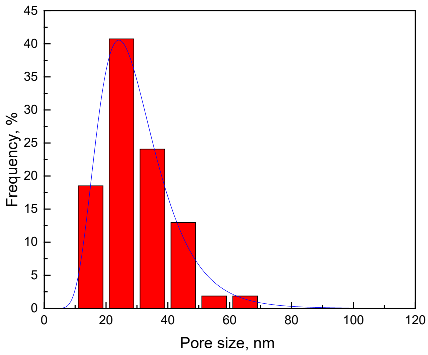


**(c)** Pore size (median) = 30 nm; σ = 12

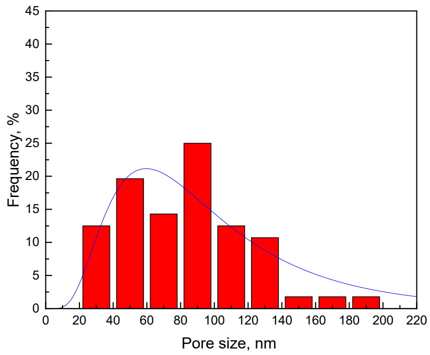


**(d)** Pore size (median) = 100 nm; σ = 64

**Figure S6.** Atomic force microscopy (AFM) images of **(a)** PVDF-TrFE/CFO and **(b)** PVDF/CFO NCs; histograms of the pore depth distribution obtained using the WSxM program for **(c)** PVDF-TrFE/CFO and **(d)** PVDF/CFO NCs. The median value and standard deviation (σ) of log-normal distribution are presented.

Topography

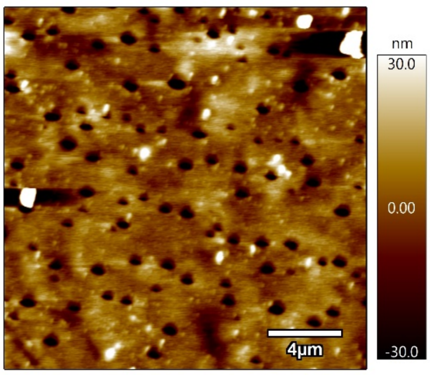


**(a)**

MFM image

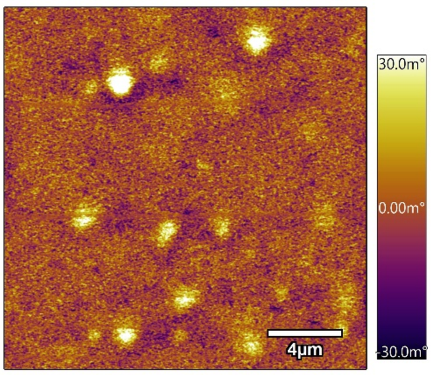


**(b)**

**Figure S7.** Magnetic force microscopy (MFM) images of PVDF-TrFE/CFO nanocomposite evaporated in the absence of magnetic field: (**a**) topology and (**b**) MFM signals.

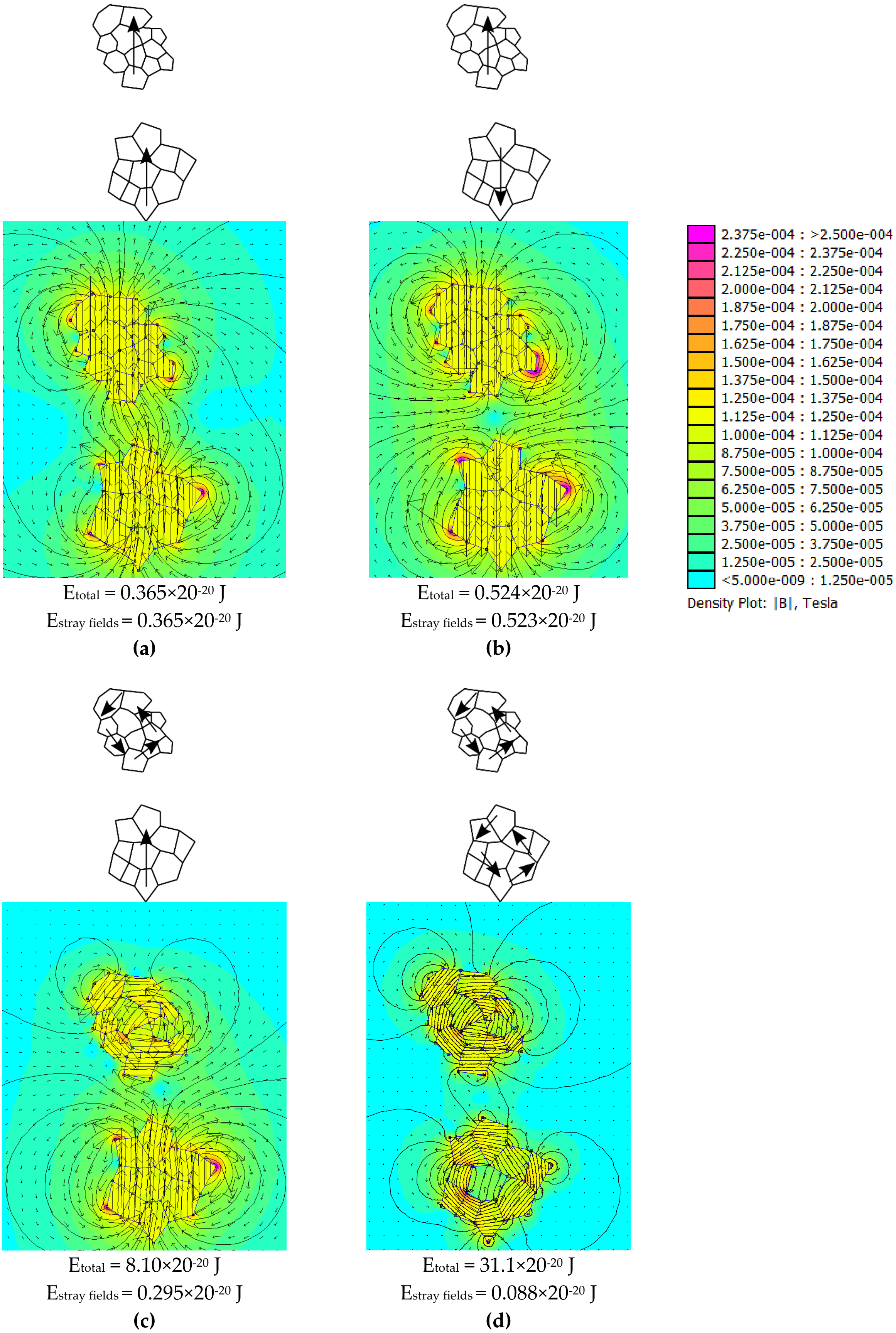


**Figure S8.** Results of FEMM simulation of magnetic induction (B) for different configurations of initial magnetization of particles aggregates: **(a)** "head-to-tail" magnetization state; **(b)** "head-to-head" magnetization state; **(c)** one aggregate has a close structure and the second is uniformly magnetized; **(d)** two aggregates have close structures.

## References


1. Peddis, D.; Jönsson, P.E.; Laureti, S.; Varvaro, G. Magnetic interactions: A tool to modify the magnetic properties of materials based on nanoparticles. In *Frontiers of Nanoscience*; Binns, C., Ed.; Elsevier B.V: Oxford, UK, 2014; Vol. 6, pp. 129–188 ISBN 9780080983530.

2. García-Otero, J.; Porto, M.; Rivas, J. Henkel plots of single-domain ferromagnetic particles. *J. Appl. Phys.* **2000**, *87*, 7376.

3. Kelly, P.E.; O'Grady, K.; Mayo, P.L.; Chantrell, R.W. Switching mechanisms in cobalt-phosphorus thin films. *IEEE Trans. Magn.* **1989**, *25*, 3881–3883.

4. Horcas, I.; Fernández, R.; Gómez-Rodríguez, J.M.; Colchero, J.; Gómez-Herrero, J.; Baro, A.M. WSXM: A software for scanning probe microscopy and a tool for nanotechnology. *Rev. Sci. Instrum.* **2007**.